ORIGINAL PAPER

Response surface methodology-based modeling and optimization of chromium removal using spiral-wound reverse-osmosis membrane setup

A. Karunakaran[1] · A. Chaturvedi[2] · J. Ali[3] · R. Singh[4] · S. Agarwal[5] · M. C. Garg[1]

Abstract

Contamination of groundwater sources due to the presence of chromium ions, a heavy metal, and the detrimental impact of it on the health of consumers have become a serious global concern. The present study was designed to understand the effects of three process variables, namely feed chromium concentration, feed pH and pressure, on chromium removal and permeate flux, by employing response surface methodology and central composite design techniques. Spiral-wound reverse-osmosis membrane was used for the removal of chromium from the groundwater samples in this study. Membrane performance, in terms of high permeate quality and flux, was evaluated by optimization of various operating conditions. The obtained experimental results were then matched with the predicted values obtained from the models. The models indicated that the highest chromium removal of 98.38% and permeate flux of 48.73 L/m^2 h could be achieved at the optimum feed pH of 3.00, pressure of 4 kg/cm^2 and feed chromium concentration of 0.431 ppm. Experimental validation confirmed that the model had higher predictive capabilities. The changes in pressure and the chromium concentration significantly affected the chromium removal and permeate flux, the former being positively correlated and the latter being negative to both the responses. Therefore, small-scale RO membranes can be used to treat aqueous solution with chromium contamination.

Keywords Central composite design · Chromium removal · Groundwater contamination · Reverse osmosis · Response surface methodology

Editorial responsibility: Parveen Fatemeh Rupani.

✉ M. C. Garg
manoj28280@gmail.com

1 Amity Institute of Environmental Sciences, Amity University Uttar Pradesh, Noida, Uttar Pradesh 201313, India

2 Department of Chemistry, DIT University, Dehradun, Uttarakhand 248009, India

3 Biological System Engineering, University of Nebraska, Lincoln, USA

4 Nebraska Water Center, University of Nebraska, Lincoln, USA

5 Department of Electronics and Communication Engineering, Motilal Nehru National Institute of Technology Allahabad, Prayagraj, Uttar Pradesh 211004, India

Introduction

Groundwater is acknowledged as essential source of drinking water, and one-third of the human population is reported to be dependent on it. Heavy metals present in groundwater are not biodegradable, hence, their treatment through the conventional means of treatment or natural processes is very unlikely. Other than that, heavy metal ions are toxic as well as carcinogenic (Kim et al. 2015; Saleh et al. 2019; Koedrith et al. 2013). Chromium (Cr), a commonly observed heavy metal contaminant, is found in surface water and groundwater due to numerous industrial activities, such as, wood preservation, textiles dyeing, leather tanning, electroplating (Kazakis et al. 2017; Mishra and Bharagava 2016; Saha et al. 2011; Sharma et al. 2008). Naturally, Cr ions concentrations in groundwater are observed to be lower than 2 µg/L but, sometimes, concentrations as high as 120 µg/L have also been reported (World Health 1996; Kazakis et al. 2017). Contamination of groundwater with Cr is a prevailing problem in countries like Brazil (Hirata and Suhogusoff 2019),

China (Guo et al. 2020), Greece (Kazakis et al. 2017), India (Poonia et al. 2021), Italy, Nigeria (Adeyemi and Ojekunle 2021), Pakistan (Raza et al. 2017), South Africa (Edokpayi et al. 2018), and USA (Coyte et al. 2020), which are well acknowledged and documented in literatures.

Cr commonly exists in two states, based on valency in water; trivalent Cr (Cr^{3+}) and hexavalent Cr (Cr^{6+}) (World Health, 2020). Cr^{3+}, nontoxic and less absorbed, is an essential trace element from nutrition point of view, and its deficiency leads to glucose intolerance, and other metabolic disorders (Zheng et al. 2015). On the other hand, Cr^{6+} is considered harmful, even in small ingestion dose. The exposure routes to Cr^{6+} are ingestion through eating, drinking, skin contact, and inhalation (Tziritis et al. 2012). The permissible limit for Cr^{6+} in drinking water is 0.05 mg/l (Standards 2012). To conclude in broad spectrum, ingestion of Cr^{6+} causes liver and kidney damage (De Rossi et al. 2018; Marikkani et al. 2019), which may sometimes be fatal. So, it is required to devise an appropriate method/ technology for the removal of Cr from water.

Many conventional treatment technologies, like ion exchange (Wang et al. 2014; Wang et al. 2020), electrolysis (Tao et al. 2014; Wang et al. 2020), solvent extraction (Ying et al. 2020), membrane separation (Muthumareeswaran et al. 2017a; Mnif et al. 2017; Taha et al. 2021) and biosorption process (Bashir et al. 2019; Yunus et al. 2020; Yadav et al. 2021), are used for the removal of heavy metal ions from the water. The Cr after treatment is generally managed by precipitating as hydrous oxide with caustic/lime soda or by incinerating it to form oxides to be disposed to landfills (Wilbur et al. 2012). All forms of inorganic ions as well as complexes of Cr are detached from water by using membrane in reverse-osmosis (RO) process. RO process involves the use of hydraulic pressure as driving force for the separation process (Rastogi 2018). Hydraulic pressure is applied in the feed side which drives the separation of ions in the feed solution and treated water (permeate) is passed through the pores in the membrane. The water through the membranes is calculated as water flux. The mechanism for Cr treatment employed in RO process is explained in Fig. 1. Application of membranes is an effective method for the removal of the prevalent Cr^{6+} and Cr^{3+} ions from the water (Muthumareeswaran et al. 2017b; Hosseini et al. 2017). However, it has some limitations such as high initial investment, operational costs and membrane fouling (Jiang et al. 2017; Garg and Joshi 2015).

Response surface methodology (RSM) is an approach which uses mathematical and statistical techniques for development of empirical model (Montgomery 2006; Jiang et al. 2013). RSM uses central composite design (CCD) of experiments to study the influence of independent (input) variables and optimize dependent (output) responses (Montgomery 2006; Schio et al. 2020). RSM focuses on modeling
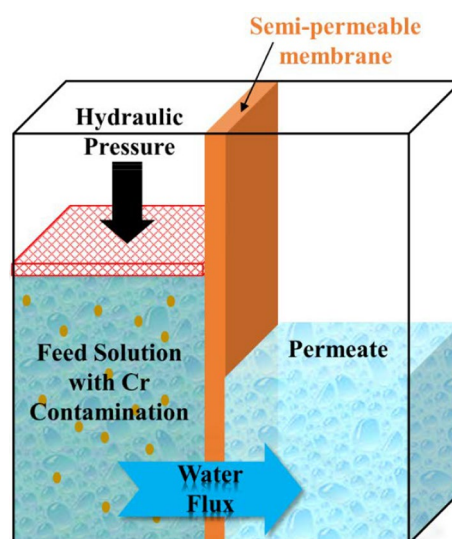
Fig. 1 Schematic figure explaining the working mechanism of RO process

experimental responses with regards to input factors (Box and Draper 1987).

Previously, RSM has been employed for the optimization of the treatment of heavy metals from water using various membrane based separation process (Rad et al. 2009; Al-Alawy and Salih 2016). It was used to model the transmembrane pressure, rejection, and recovery for ultra-filtration, nanofiltration and RO membranes. However, limited progress has been reported using small-scale RO membrane by employing RSM, which can save initial capital costs to treat groundwater with Cr contamination. Therefore, this study was conducted to model the performance and optimization of small-scale RO membrane for the operating parameters like Cr concentration, feed pH and pressure for maximizing Cr removal and permeate flux. Further, we have carried out kinetics study to determine the change in Cr concentration over time to validate the optimum results from the models. The experiments were carried out in Amity Institute of Environmental Sciences, Amity University-Noida, India.

Materials and methods

RO membrane setup and operating procedure

A laboratory-scale RO membrane system was used to model the removal of Cr from aqueous solution. Figure 2 shows the schematic diagram of the laboratory-scale spiral-wound RO setup used in this study. It comprised of feed tank, pressure pump, membrane cell, and a RO membrane in spiral-wound configuration. Commercially available domestic-RO
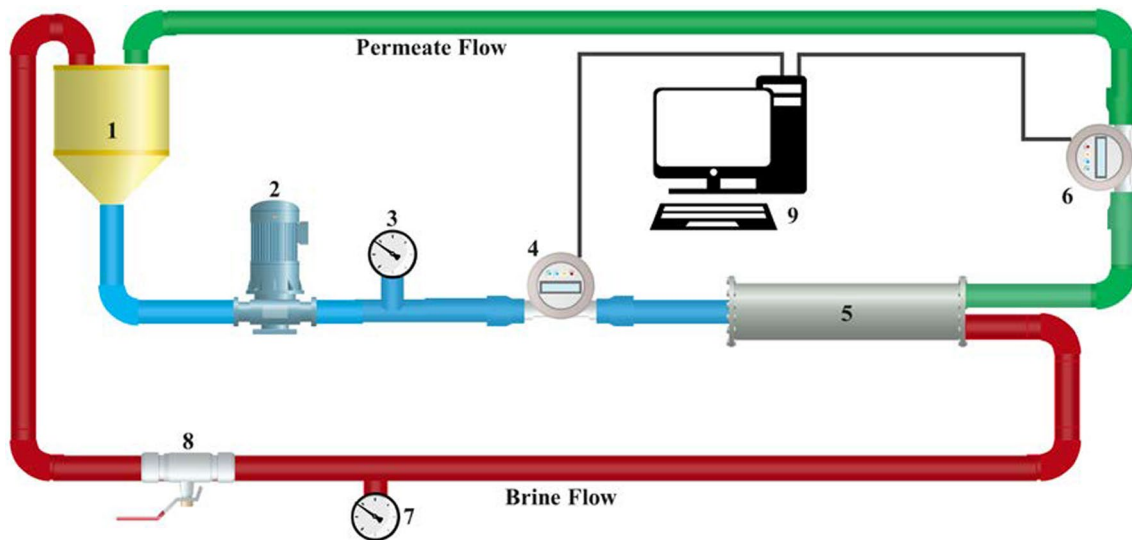
Fig. 2 Schematic diagram of small-scale spiral-wound reverse-osmosis (RO) membrane setup; 1—feed tank containing Cr aqueous solution, 2—Pressure pump, 3—Feed flow pressure gauge, 4—feed flow meter, 5—RO spiral-wound membrane cell, 6—Permeate flow meter, 7—Brine flow pressure gauge, 8—Pressure control valve, 9—Computer for data logging

membrane (Make: CSM, Model: RE1812-80) was used in this study.

In this study, synthetically prepared Cr water (a known concentration of Cr) was applied as feed water to check the membrane performance. The flow rate at the feed side was kept uniform throughout the experiments. Pressure pump was used to provide the necessary operating pressure to the system which was regulated with the help of a pressure control valve. Pressure gauges flow meters were provided to monitor the pressure and flow rate of the system, respectively. Flow meters were connected to micro-processors for logging the data, to be used for the calculation of the permeate flux. After the experiments were conducted, initially, the membranes were back-flushed with distilled water followed by forward flushing with 1% sodium metabisulfite solution until the RO module was completely replaced with it.

Groundwater samples were collected from three locations (L_1, L_2 and L_3) in Delhi-NCR, India and were analyzed for its physical and chemical parameters. The details are shown in Table 1 and have been compared with the acceptable and permissible limits from BIS 10500:2012 (Standards 2012). Though the Cr concentration from these locations was within the acceptable limit, higher Cr concentrations have been reported earlier (Shekhar and Sarkar 2013).

The feed and permeate stream concentrations of Cr were measured with the help of Spectrophotometer (Make: *Labman Scientific Instruments Pvt. Ltd., India*), following standard methods (Baird and Bridgewater 2017). Spectrophotometric analysis was conducted at the wavelength of 540 nm, using a light path passing through a 1 cm cuvette. For the analysis of Cr concentration, a calibration curve

was prepared and plotted with observed absorbance values against known Cr concentration. The Cr ions concentrations of the water samples were then calculated using the linear equation obtained from the calibration curve. Cr removal (%) was estimated using Eq. (1):

$$\text{Cr removal}(\%) = \frac{(C_0 - C_t)}{C_0} \times 100 \tag{1}$$

where C_0 is the initial Cr concentration in feed solution (mg/L) and C_t is the final Cr concentration in the permeate (mg/L).

Permeate flux in L/m^2 h (LMH) was calculated as per Eq. (2) shown below:

$$\text{Permeate Flux} = \frac{q_p}{A_m} \tag{2}$$

where q_p is permeate flow rate (L/hr) and A_m is area of membrane (m^2).

Feed solution pH was maintained using 1 M NaOH and 1 M HCl solutions. It was measured with the help of calibrated pH meter (Make: *Hach Inc., USA*, Model: *HQ40d*).

CCD of experiments

A full-factorial CCD was used for developing mathematical equations, in terms of percentage removal of Cr, and permeate flux, providing quantifiable assessment of membrane system to treat Cr contaminated water samples. Membrane performance, in terms of high permeate quality, and flow rate, was evaluated by optimizing various

Table 1 Physical and Chemical parameters of groundwater

Parameters	Unit	L_1	L_2	L_3	As per BIS 10500:2012	
					Acceptable limit	Permissible Limit
pH		7.45	7.30	7.44	6.5–8.5	NR
Temp	^{o}C	27.70	27.70	28.00	–	–
EC	µS/cm	6180	3910	16,170	–	–
Turbidity	NTU	1.56	0.44	1.43	5	10
BOD_5	mg/L	1.30	1	1.40	–	–
COD	mg/L	4	16	44	–	–
TKN	mg/L	0	0	0.11	–	–
Alkalinity	mg/L	34	62	24	200	600
Hardness	mg/L	1480	720	4000	300	600
TDS	mg/L	4456	2404	12,450	500	2000
TSS	mg/L	192	76	22	–	–
TS	mg/L	4648	2480	12,472	–	–
Sodium (Na^+)	mg/L	745.70	457.75	1999.8	–	–
Potassium (K^+)	mg/L	0	12.61	0	–	–
Calcium (Ca^{2+})	mg/L	452.55	160.95	941.60	75	200
Magnesium (Mg^{2+})	mg/L	156.50	92.95	621.60	30	100
Fluoride (F^-)	mg/L	0.50	1.49	1.35	1	2
Chloride (Cl^-)	mg/L	1951.95	713.20	5200	250	1000
Nitrate (NO_3^-)	mg/L	47	40.75	126.30	45	NR
Sulfate (SO_4^{2-})	mg/L	538.72	315.39	676.45	200	400
Iron (Fe^{2+})	mg/L	0.62	0.23	0.88	0.3	1
Manganese (Mn^{2+})	mg/L	0	0.03	0.06	0.1	0.3
Arsenic (As^{3+})	mg/L	0.01	0	0.02	0.01	NR
Lead (Pb^{2+})	mg/L	0.01	0	0	0.05	NR
Chromium (Cr^{2+})	mg/L	0	0.01	0	0.05	NR
Selenium (Se^{2-})	mg/L	0.02	0.01	0.09	0.01	NR
Boron (B^{3+})	mg/L	0.01	0.03	0.02	1	5

operating variables such as feed pressure, feed pH and Cr concentration in feed solution.

To study the effects of three process variables simultaneously, CCD of RSM was selected. Both linear and quadratic models were used to determine the Cr removal and permeate flux. The general form of second-order model can be expressed according to Eq. (3):

$$y = \beta_0 + \sum_{i=1}^{n} \beta_i x_i + \sum_{i=1}^{n} \beta_{ii} x_i^2 + \sum_{i<j} \sum \beta_{ij} x_i x_j + \varepsilon \quad (3)$$

where y is the response, x_i is coded levels of operating variables; β_0, β_i, β_{ii} and β_{ij} are the regression coefficients for constant term, linear, quadratic and interaction parameters, respectively; n is number of operating variables and ε is experimental error (K et al. 2021; Aghilesh et al. 2021). To establish its statistical implication, analysis of variance (ANOVA) for the model was also carried out. Design-Expert

(*Stat-Ease Inc., USA*) software was used for design of experiments and for statistical and graphical data analysis.

In the present study, after a careful analysis of literature, concentration of Cr (Hafez and El-Mariharawy 2004), feed pH and feed pressure (Gasemloo et al. 2019; Hafez and El-Mariharawy 2004) were chosen as input variables for the optimization of RO system. A full factorial design of the factors with various ranges were considered as shown in Table 2. A total of 19 experimental sets were designed with the use of software according to Eq. (4). The experimental sets comprise of eight cubical or factorial points, six axial points, and five repetition of center points.

$$N = 2^n + 2n + n_c \quad (4)$$

where N is the required total number of experiments, n is the number of operating variables and n_c is replicate number at the center points (Sen et al. 2018; Garg and Joshi 2017).

Table 2 Range and levels of operating variables for CCD ($\alpha = \pm 1.68$)

Operating Variables	Code	Coded levels and ranges				
		$-\alpha$	-1	0	$+1$	$+\alpha$
Cr concentration (ppm)	A	0.10	0.30	0.50	0.70	0.90
Feed pH	B	2	3	4	5	6
Feed pressure (kg/cm^2)	C	1	2	3	4	5

Results obtained were subjected to ANOVA, later being utilized for the graphical analysis of the data. This gives the interaction between the responses and the variables.

Kinetics study

Kinetics study was carried out to investigate the change in feed and permeate stream over time. For this study, the experiments were carried out by recirculating the brine flow to the feed stream and collecting the permeate flow separately. The impacts of pressure and Cr concentration were studied for both the feed and permeate stream. A total of 5 L of feed Cr solution was prepared, and the experiments were carried out until the feed stream was filtered toward the permeate stream. The Cr concentrations in feed and permeate streams were continuously monitored. The pressure and Cr concentration were selected from -1, 0

and $+1$ range from Table 2. Further, the optimum pressure and Cr concentration obtained from RSM optimization were used to validate the results.

Results and discussion

Table 3 shows the CCD matrix of experiments with its responses for Cr removal and permeate flux. The operating variables in Table 3 are shown in terms of codded levels according to Table 2. All the experiments were carried out in accordance with the CCD of experiments and observed responses; Cr removal (%) and permeate flux (LMH) were calculated using Eqs. (1) and (2), respectively. Also, predicted responses obtained from the models are also shown in Table 3.

Table 3 CCD matrix with predicted and observed responses for Cr removal and permeate flux

Operating variables			Responses			
A	B	C	Cr removal (%)		Permeate flux (LMH)	
			Observed	Predicted	Observed	Predicted
-1	-1	-1	97.6	97.3	24.8	24.6
$+1$	-1	-1	97.2	97.0	24.7	24.4
-1	$+1$	-1	97.0	96.7	24.7	24.6
$+1$	$+1$	-1	96.7	96.5	24.6	24.4
-1	-1	$+1$	98.4	98.1	48.7	47.5
$+1$	-1	$+1$	98.1	97.8	48.4	47.1
-1	$+1$	$+1$	97.9	97.7	48.4	47.3
$+1$	$+1$	$+1$	97.8	97.5	48.1	46.9
$+\alpha$	0	0	96.2	96.5	35.7	36.5
$-\alpha$	0	0	97.8	98.1	36.6	37.2
0	$+\alpha$	0	97.4	97.7	36.2	36.8
0	$-\alpha$	0	96.9	97.2	36.2	37.0
0	0	$+\alpha$	98.6	98.8	54.1	55.8
0	0	$-\alpha$	94.6	94.8	10.8	10.4
0	0	0	97.6	97.7	36.4	36.6
0	0	0	97.6	97.7	36.3	36.6
0	0	0	97.6	97.7	36.4	36.6
0	0	0	97.6	97.7	36.3	36.6
0	0	0	97.6	97.7	36.4	36.6

where A is Cr concentration in feed solution (ppm), B is pH of feed solution and C is feed pressure (kg/cm^2)

Table 4 ANOVA results for Cr removal model and permeate flux model

Source	Sum of squares	df	Mean square	F value	p value
Cr removal model					
Linear	1.33	1	1.33	8.69	0.022
Interaction	1.19	1	1.19	7.77	0.027
Square	1.05	1	1.05	6.89	0.034
Residual	1.07	7	0.15		
Permeate flux model					
Linear	2061.95	1	2061.95	1643.46	< 0.0001
Interaction	0.03	1	0.03	0.02	0.8857
Square	18.06	1	18.06	14.40	0.0043
Residual	11.29	9	1.25		

where df is degrees of freedom

Table 5 Statistical analysis for Cr removal and permeate flux models

Statistical Indices	Models	
	Cr removal	Permeate flux
R^2	0.9238	0.9946
$R^2_{adjusted}$	0.8031	0.9892
MSE	0.0560	0.5943
RMSE	0.2367	0.7709
MAE	0.2255	0.6158

Response surface modeling for Cr removal

Suitability of the model was evaluated with the use of ANOVA (Gasemloo et al. 2019). The experimental responses were used to analyze the data. Significance of the data and coefficient of determination (R^2) were estimated using ANOVA. Also, statistical indices like correlation coefficient (R), mean squared error (MSE), root-mean-squared error (RMSE) and mean average error (MAE) were calculated to determine the precision of the model. Table 4 shows the ANOVA table for Cr removal and permeate flux.

$$
\begin{aligned}
\text{Chromium Removal} =\ & 97.68 - 0.41A + 0.12B + 1.00C + 0.01AC \\
& + 0.04BC - 0.10A^2 - 0.06B^2 - 0.21C^2 \\
& - 0.55A^2C + 0.29AC^2 - 0.36BC^2
\end{aligned}
\tag{5}
$$

where A, B and C are coded factors, Cr concentration, feed pH and feed pressure. AB, BC & AC are the interactive terms. A^2C, AC^2 and BC^2 are the quadratic terms. From Table 4, F value of 7.680 specifies that the model terms are significant and there is only 0.620% chance for the model to have larger F value which occurs due to noise. The p value of the linear, interaction and square terms were < 0.050, which indicates the model to be significant, while p value of lack of fit was > 0.050, which indicates that it is insignificant (Singh et al. 2019a). This shows that the model can be used to predict the Cr removal.

Also, from Table 5 R^2 and $R^2_{adjusted}$ values were calculated as 0.9238 and 0.8031, respectively. Higher values confirm the model agrees with the experimental results. MSE, RMSE and MAE was found to be 0.0560, 0.2367 and 0.2255, respectively. Lower values of MSE, RMSE and MAE can be attributed to better accuracy and precision of the model to predict the Cr removal.

Graphical analysis of the data was represented in terms of 3D response surface plots. These plots graphically describe the interactive effects of independent variables (Gasemloo et al. 2019; Khayet et al. 2011; Kassem et al. 2017) on the Cr removal (%). Figure 3d shows the predicted and actual plots for Cr removal. This indicates the accuracy and reliability of the model.

The response plot in Fig. 3b indicates that the Cr removal is affected very slightly with the change of feed pH. At higher feed pressure, the increase in pH has a slight decrease in Cr removal (%) (Thilagavathy and Santhi 2013; Gasemloo et al. 2019; Khalifa et al. 2019). However, the change of pH has lower change in the Cr removal (%) from water. However, Cr removal (%) increases with the increase in pressure (Fig. 3a, c). This is because at lower pressure, the diffusion of Cr ions is lower (Wei et al. 2013; Basaran et al. 2016). Therefore, as the pressure increases, we can observe a higher Cr removal (%). This indicates higher removal of Cr at higher pressures. But, as the Cr concentration in the feed increases, the Cr removal (%) slightly decreases for all pressure ranges. This happens because the osmotic pressure is a function of the concentration of salts or organics present in the feed solution. Figure 3d indicates that the predictions did hold true as actual values are either seen to fall on the same line or closely scattered around.

Response surface modeling for permeate flux

Tables 4 and 5 show the ANOVA results along with statistical indices like R, R^2, MSE, RMSE and MAE with regard to Cr removal and permeate flux models. The analysis shows that the model terms are significant.

$$
\begin{aligned}
\text{Permeate Flux} =\ & 36.62 - 0.16A - 0.05B + 11.35C \\
& + 0.01AB - 0.06AC - 0.05BC \\
& + 0.05A^2 - 0.06B^2 - 0.87C^2
\end{aligned}
\tag{6}
$$

where A, B and C are coded factors, Cr concentration, feed pH and feed pressure. AB, BC and AC are the interaction terms. From Table 4, F value of linear terms of the model shows that model terms are significant and there is $< 0.01\%$ chance for the model to have larger F value which occurs due to noise (Singh et al. 2019b). The p values of linear and square terms were < 0.050, which indicates the model to be

Fig. 3 Response surface 3D plots for (**a**) interactive effect of feed Cr concentration and feed pressure, (**b**) feed pH and feed Cr concentration, (**c**) Contour plot for feed pressure and feed Cr concentration, (**d**) predicted vs. actual plots for Cr removal (%)
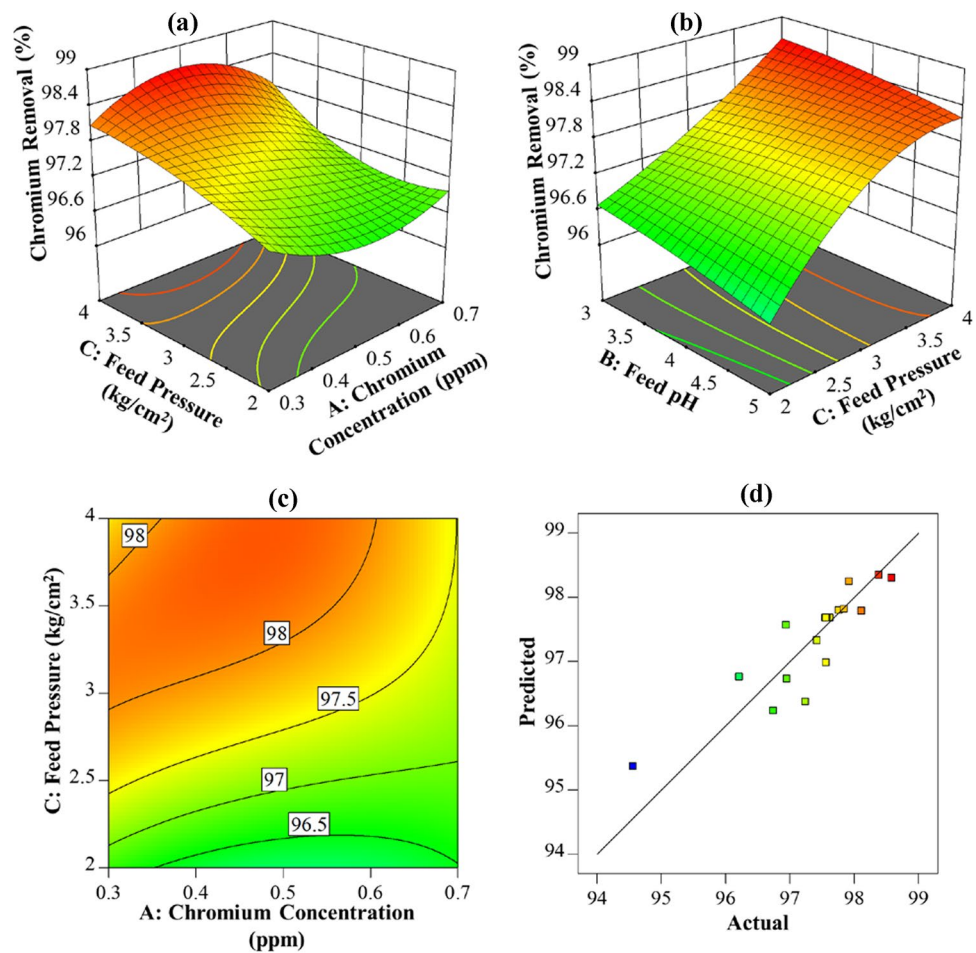
significant and p-vale of lack of fit was > 0.050, which is insignificant. Permeate flux model can the flux generated for the Cr removal.

Also, from Table 5 R^2 and $R^2_{adjusted}$ values were calculated as 0.9946 and 0.9892, respectively and its higher values confirm the model with experimental results. Further, MSE, MSE and MAE was calculated as 0.5943, 0.7709 and 0.6158, respectively as shown in Table 5, which determines the precision of the model for predicting the permeate flux. Figure 4d shows the predicted and actual plots for Cr removal. This indicates the accuracy and reliability of the model. This plot shows an acceptable agreement between observed data and those predicted from the model.

The response plot (Fig. 4a) indicates that a decrease or increase in the pH of the feed solution do not affect the permeate flux. Whereas on increasing the pressure, the permeate flux increases gradually. The response plot (Fig. 4b, c) shows that the effect of Cr concentration in the feed solution has a very slight effect on the flux. The increase in the concentration slightly decreases the permeate flux of the system at all values of pressure. This happens because higher Cr concentration in the feed results in lower membrane flux at

a constant pressure. From Fig. 4d, it can be concluded that the actual and predicted values were in good agreement.
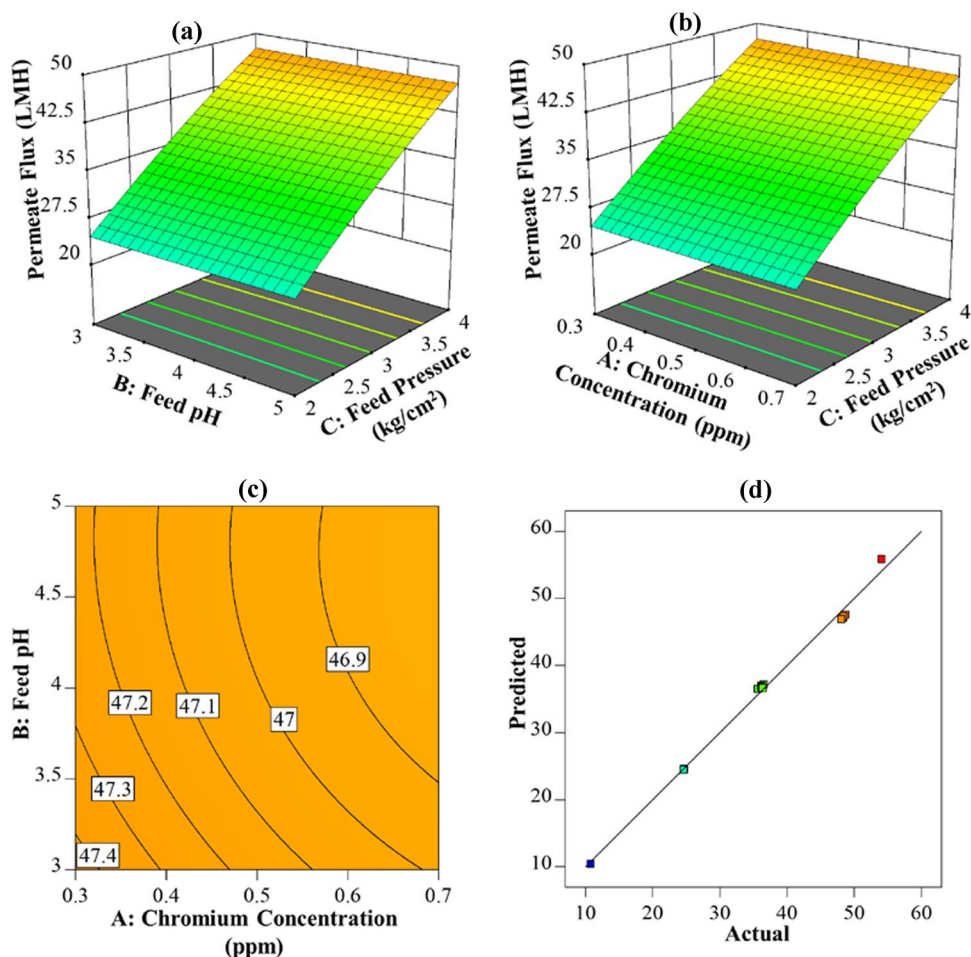
Multiparameter optimization of Cr removal

The main aim of this study was to use experimental design for optimization of Cr removal from aqueous solution. The optimization of was carried out using Design Expert software by setting the criteria of maximizing Cr removal (%) and permeate flux (LMH) while targeted values of three independent variables were selected within the range for the experiment.

The optimum conditions for maximum Cr removal and permeate flux with the use of RO membrane in this study are shown in Table 6. These running conditions will provide with the best permeate quality in terms of Cr removal (%) and the permeate flux. To validate the results, additional experiments were carried out with the optimal parameters and the results are presented in Table 6. The difference in the predicted and actual results for Cr removal and water flux was 0.2% and 2.92%, respectively. Also, Cr concentration was found to be within the permissible limit in drinking water i.e., 0.05 mg/l (Standards 2012). The flux will also be

Fig. 4 Response surface 3D plots for (**a**) interactive effect of feed pH and feed pressure, (**b**) feed pressure and feed Cr concentration, (**c**) contour plot for feed pH and feed Cr concentration, (**d**) predicted vs. actual plots for permeate flux (LMH)

Table 6 Multiparameter optimization results with experimental results

	Cr concentration ppm	Feed pH –	Pressure kg/cm^2	Cr removal %	Permeate flux LMH
Predicted	0.431	3	4	98.58	47.35
Actual				98.38	48.73
Percentage difference of predicted and actual				0.20%	2.92%

maximized under these run conditions hence maximizing the output of the RO system. This will help us obtain the maximum amount of permeate in the given time thereby boosting the RO efficiency and reducing the input investment costs.

Kinetics study

The change in Cr concentrations in both feed and permeate streams at 2 and 4 kg/cm^2 of applied pressure is shown in Fig. 5. It can be observed that in feed stream, Cr concentration increases at a faster rate at 4 kg/cm^2 pressure, compared to that of 2 kg/cm^2 pressure (Fig. 5a). From Fig. 5b, it is shown that at 4 kg/cm^2 pressure Cr concentration was found below acceptable limit of 0.05 ppm (Standards 2012) than

the 2 kg/cm^2 applied pressure, this may be because the rejection of ions increases with increase in pressure (Garg and Joshi 2017; Srivastava et al. 2021). Further, at the optimum pressure of 4 kg/cm^2, permeate stream was found to be well below the acceptable limit of Cr (Fig. 5b), thus validating the results obtained from Table 6.

Also, experiments were carried out at various feed Cr Concentrations while keeping the other operating factors according to Table 6. Figure 6 shows the change of feed and permeate Cr concentrations at 0.3, 0.5, 0.7 and 0.431 ppm. The trend of Cr concentration in feed and permeate stream was found to be identical. The feed Cr concentration was highest at initial Cr concentration of 0.7 ppm (Fig. 6a). While in permeate stream, the Cr concentration was below the acceptable limit
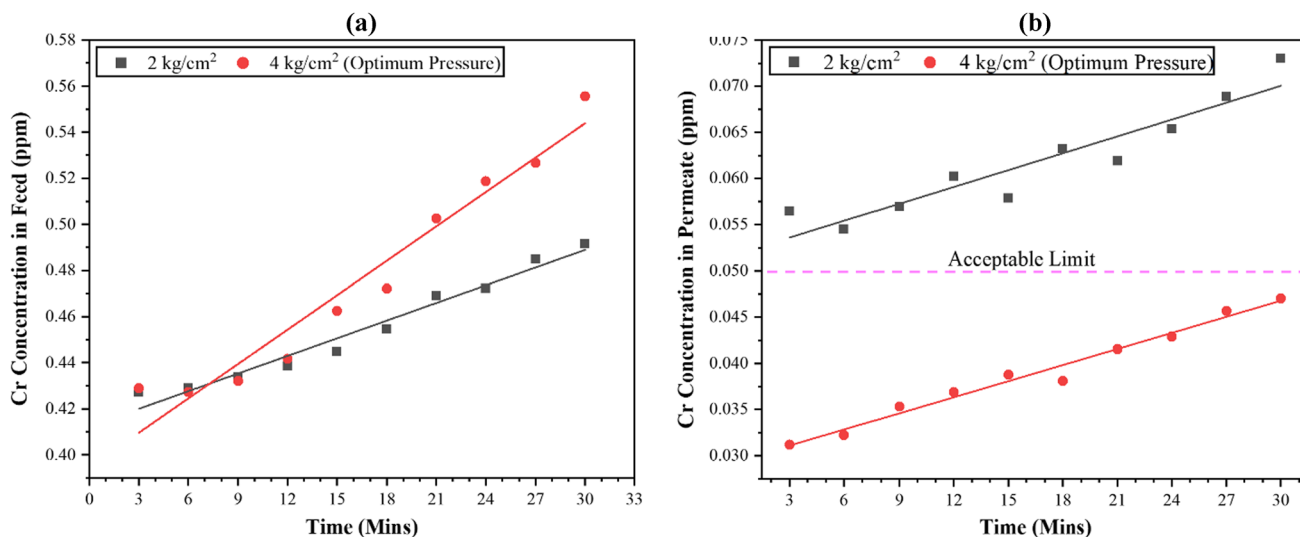
Fig. 5 Change in Cr concentration in (**a**) feed and (**b**) permeate streams (at feed Cr concentration = 0.431 ppm and pH = 3)
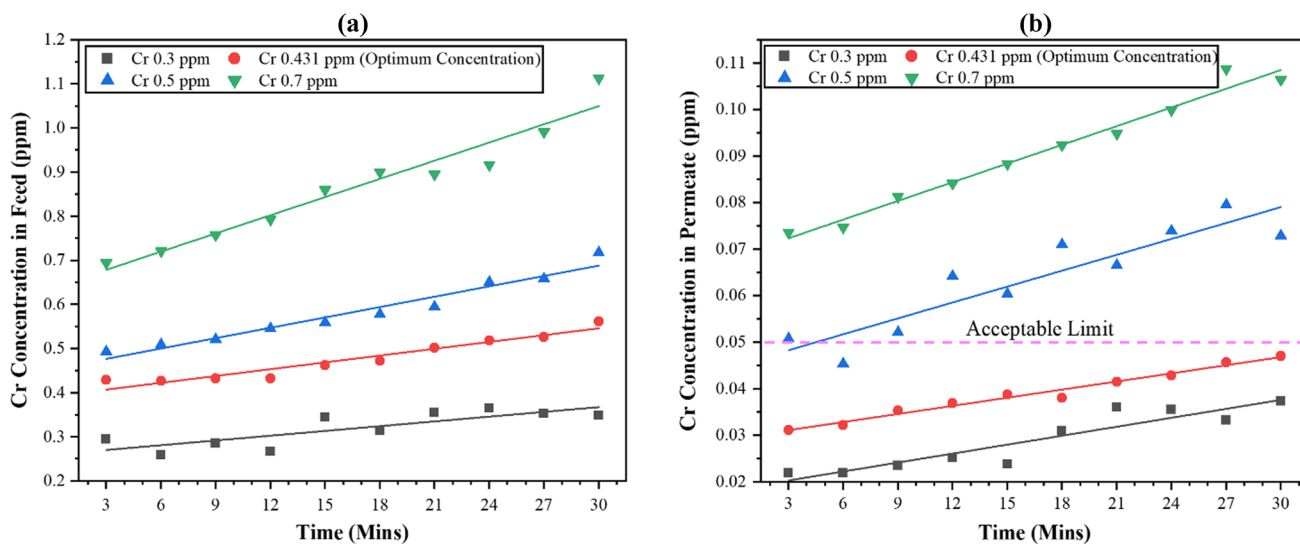

Fig. 6 Change in Cr concentration in (**a**) feed and (**b**) permeate (at feed pressure = 4 kg/cm^2 and pH = 3)

at optimum feed Cr concentration of 0.431 ppm (Fig. 6b), thereby, justifying the optimization results (Table 6) obtained by the RSM model.

Also, Table 7 shows the comparison of Cr removal by various membrane types with the present study. This comparison data reveals that among various membrane types, the small-scale RO membranes used in the current study can facilitate highest removal of Cr from waters.

Conclusion

In this study, CCD of RSM was chosen to model the effects of three process variables: Cr concentration, feed pH and pressure, for two responses: Cr removal (%) and permeate flux. The optimal conditions for operating variables were at pH at 3, pressure of 4 kg/cm^2 and Cr concentration

Table 7 Comparison of Cr removal by various methods

Membrane type	Material/Make	Cr removal (%)	Reference
Nanofiltration	Hollow fiber	95.76	Wei et al. (2013)
Nanofiltration	Dow Filmtec (NF90)	97.00	Piedra et al. (2015)
Nanofiltration	Polyamide	94.00	Basaran et al.(2016)
RO	AG membranes	91%	Çimen (2015)
RO	Polyamide Thin film composite	97.7	Mnif et al. (2017), Ozaki et al. (2002)
RO	CSM (RE1812-80)	98.58	Present study

of 0.431 ppm, resulting into a higher Cr removal rate of 98.38% and the higher permeate flux of 48.73 LMH. The results were compared with the predictions of the models and only had less than 3% difference. The predictive capability of the regression models was found to be higher and was statistically with R^2 values 0.9238 and 0.9946 for Cr removal and permeate flux models, respectively. From the interactive plots, it was observed that the increase in the operating pressure to 4 kg/cm^2, increased Cr removal and permeate flux. Similarly, increase in the concentration of the feed was observed the decrease the Cr removal and a slight decrease in permeate flux. Based upon the observed results and the stability of the developed models, it could be concluded that the RO membranes can facilitate higher Cr removal with a high permeate flux, resulting into higher volume of water reclamation within the same input investment cost. Cr in groundwater can be remediated by reduction of Cr^{6+} to Cr^{3+} and precipitated as hydroxides. Natural attenuation can also be carried out by the similar principle if natural reductants are present in the groundwater. However, some future scope of actions are worth consideration for promoting its application, which are (a) inclusion of other operating parameters like temperature, recovery and energy consumption of membrane process for the performance optimization of RO system, (b) extension of similar approach for the treatment of aqueous solution contaminants including various other heavy metals like arsenic, cadmium, lead, and (c) similar optimization studies on various types of membranes separation techniques like ultrafiltration, nanofiltration to do a comparative study.

Declarations

Conflict of interest The authors declare that they have no known competing financial interests or personal relationships that could have appeared to influence the work reported in this paper.

References

Adeyemi AA, Ojekunle ZO (2021) Concentrations and health risk assessment of industrial heavy metals pollution in groundwater in Ogun state, Nigeria. Sci African 11:e00666

Aghilesh K, Mungray AA, Agarwal S, Garg MC (2021) Optimization of forward-osmosis performance with low-concentration draw solution using response surface modelling. Chem Eng Technol. https://doi.org/10.1002/ceat.202000453

Al-Alawy AF, Salih MH (2016) Theoretical and experimental study of nano filtration and reverse osmosis membranes for removal of heavy metals from wastewater. Int J Sci Res 6:778–788

Baird R, Bridgewater L (2017) Standard methods for the examination of water and wastewater. American Public Health Association, Washington D.C

Basaran G, Kavak D, Dizge N, Asci Y, Solener M, Ozbey B (2016) Comparative study of the removal of nickel(II) and chromium(VI) heavy metals from metal plating wastewater by two nanofiltration membranes. Desalin Water Treat 57:21870–21880

Bashir A, Malik LA, Ahad S, Manzoor T, Bhat MA, Dar GN, Pandith AH (2019) Removal of heavy metal ions from aqueous system by ion-exchange and biosorption methods. Environ Chem Lett 17:729–754

Box GEP, Draper NR (1987) Empirical model-building and response surfaces. Wiley

World Health O (2020) Chromium in drinking-water. World Health Organization

Çimen A (2015) Removal of chromium from wastewater by reverse osmosis. Russ J Phys Chem A 89:1238–1243

Coyte RM, Mckinley KL, Jiang S, Karr J, Dwyer GS, Keyworth AJ, Davis CC, Kondash AJ, Vengosh A (2020) Occurrence and distribution of hexavalent chromium in groundwater from North Carolina, USA. Sci Total Environ 711:135135

de Rossi A, Rigon MR, Zaparoli M, Braido RD, Colla LM, Dotto GL, Piccin JS (2018) Chromium (VI) biosorption by Saccharomyces cerevisiae subjected to chemical and thermal treatments. Environ Sci Pollut Res 25:19179–19186

Edokpayi JN, Enitan AM, Mutileni N, Odiyo JO (2018) Evaluation of water quality and human risk assessment due to heavy metals in groundwater around Muledane area of Vhembe District, Limpopo Province, South Africa. Chem Cent J 12:2

Garg MC, Joshi H (2015) Optimization and economic analysis for a small scale nanofiltration and reverse osmosis water desalination system. Water Supply 15:1027–1033

Garg MC, Joshi H (2017) Comparative assessment and multivariate optimization of commercially available small scale reverse osmosis membranes. J Environ Inf 29:39–52

Gasemloo S, Khosravi M, Sohrabi MR, Dastmalchi S, Gharbani P (2019) Response surface methodology (RSM) modeling to improve removal of Cr (VI) ions from tannery wastewater

using sulfated carboxymethyl cellulose nanofilter. J Clean Prod 208:736–742

World-Health O (1996) Guidelines for drinking-water quality. 2nd edn, vol 2 Health criteria and other supporting information. WHO, Geneva

Guo H, Chen Y, Hu H, Zhao K, Li H, Yan S, Xiu W, Coyte RM, Vengosh A (2020) High hexavalent chromium concentration in groundwater from a deep aquifer in the Baiyangdian Basin of the North China Plain. Environ Sci Technol 54:10068–10077

Hafez A, El-Mariharawy S (2004) Design and performance of the two-stage/two-pass RO membrane system for chromium removal from tannery wastewater: part 3. Desalination 165:141–151

Hirata R, Suhogusoff AV (2019) How much do we know about the groundwater quality and its impact on Brazilian society today? Acta Limnologica Brasiliensia. 31

Hosseini SS, Nazif A, Shahmirzadi MAA, Ortiz I (2017) Fabrication, tuning and optimization of poly (acrilonitryle) nanofiltration membranes for effective nickel and chromium removal from electroplating wastewater. Sep Purif Technol 187:46–59

Standards BOI (2012) IS 10500: drinking water: specification (Second Revision). New Delhi, India: Bureau of Indian Standards

Jiang W, Joens JA, Dionysiou DD, O'Shea KE (2013) Optimization of photocatalytic performance of TiO2 coated glass microspheres using response surface methodology and the application for degradation of dimethyl phthalate. J Photochem Photobiol, A 262:7–13

Jiang S, Li Y, Ladewig BP (2017) A review of reverse osmosis membrane fouling and control strategies. Sci Total Environ 595:567–583

Mungray KA, Agarwal A, Ali S, Chandra-Garg J (2021) Performance optimisation of forward-osmosis membrane system using machine learning for the treatment of textile industry wastewater. J Clean Prod 289:125690

Kassem Y, Çamur H, Esenel E (2017) Adaptive neuro-fuzzy inference system (ANFIS) and response surface methodology (RSM) prediction of biodiesel dynamic viscosity at 313 K. Procedia Comput Sci 120:521–528

Kazakis N, Kantiranis N, Kalaitzidou K, Kaprara E, Mitrakas M, Frei R, Vargemezis G, Tsourlos P, Zouboulis A, Filippidis A (2017) Origin of hexavalent chromium in groundwater: the example of Sarigkiol Basin, Northern Greece. Sci Total Environ 593–594:552–566

Khalifa EB, Rzig B, Chakroun R, Nouagui H, Hamrouni B (2019) Application of response surface methodology for chromium removal by adsorption on low-cost biosorbent. Chemom Intell Lab Syst 189:18–26

Khayet M, Cojocaru C, Essalhi M (2011) Artificial neural network modeling and response surface methodology of desalination by reverse osmosis. J Membr Sci 368:202–214

Kim HS, Kim YJ, Seo YR (2015) An overview of carcinogenic heavy metal: molecular toxicity mechanism and prevention. J Cancer Prev 20:232–240

Koedrith P, Kim H, Weon J-I, Seo YR (2013) Toxicogenomic approaches for understanding molecular mechanisms of heavy metal mutagenicity and carcinogenicity. Int J Hyg Environ Health 216:587–598

Marikkani S, Kumar JV, Muthuraj V (2019) Design of novel solar-light driven sponge-like Fe2V4O13 photocatalyst: a unique platform for the photoreduction of carcinogenic hexavalent chromium. Sol Energy 188:849–856

Mishra S, Bharagava RN (2016) Toxic and genotoxic effects of hexavalent chromium in environment and its bioremediation strategies. J Environ Sci Health C 34:1–32

Montgomery DC (2006) Design and analysis of experiments. Wiley

Mnif A, Bejaoui I, Mouelhi M, Hamrouni B (2017) Hexavalent chromium removal from model water and car shock absorber factory effluent by nanofiltration and reverse osmosis membrane. Int J Anal Chem 2017:7415708

Muthumareeswaran MR, Alhoshan M, Agarwal GP (2017a) Ultrafiltration membrane for effective removal of chromium ions from potable water. Sci Rep 7:41423

Muthumareeswaran MR, Alhoshan M, Agarwal GP (2017b) Ultrafiltration membrane for effective removal of chromium ions from potable water. Sci Rep 7:1–12

Ozaki H, Sharma K, Saktaywin W (2002) Performance of an ultra-low-pressure reverse osmosis membrane (ULPROM) for separating heavy metal: effects of interference parameters. Desalination 144:287–294

Piedra E, Álvarez JR, Luque S (2015) Hexavalent chromium removal from chromium plating rinsing water with membrane technology. Desalin Water Treat 53:1431–1439

Poonia T, Singh N, Garg MC (2021) Contamination of Arsenic, Chromium and Fluoride in the Indian groundwater: a review, meta-analysis and cancer risk assessment. Int J Environ Sci Technol 289:125690

Rastogi NK (2018) Chapter 13: reverse osmosis and forward osmosis for the concentration of fruit juices. In: Rajauria G, Tiwari BK (eds) Fruit juices. Academic Press, San Diego

Rad SAM, Mirbagheri SA, Mohammadi T (2009) Using reverse osmosis membrane for chromium removal from aqueous solution. World Acad Sci Eng Technol 3:348–352

Raza M, Hussain F, Lee J-Y, Shakoor MB, Kwon KD (2017) Groundwater status in Pakistan: a review of contamination, health risks, and potential needs. Crit Rev Environ Sci Technol 47:1713–1762

Saha R, Nandi R, Saha B (2011) Sources and toxicity of hexavalent chromium. J Coord Chem 64:1782–1806

Saleh HN, Panahande M, Yousefi M, Asghari FB, Oliveri-Conti G, Talaee E, Mohammadi AA (2019) Carcinogenic and non-carcinogenic risk assessment of heavy metals in groundwater wells in neyshabur plain, Iran. Biol Trace Element Res 190:251–261

Schio RR, Salau NPG, Mallmann ES, Dotto GL (2020) Modeling of fixed-bed dye adsorption using response surface methodology and artificial neural network. Chem Eng Commun 14:1–12

Sen S, Nandi S, Dutta S (2018) Application of RSM and ANN for optimization and modeling of biosorption of chromium(VI) using cyanobacterial biomass. Appl Water Sci 8:148

Sharma SK, Petrusevski B, Amy G (2008) Chromium removal from water: a review. J Water Supply Res Technol AQUA 57:541–553

Shekhar S, Sarkar A (2013) Hydrogeological characterization and assessment of groundwater quality in shallow aquifers in vicinity of Najafgarh drain of NCT Delhi. J Earth Syst Sci 122:43–54

Singh R, Bhunia P, Dash RR (2019a) Optimization of bioclogging in vermifilters: A statistical approach. J Environ Manag 233:576–585. https://doi.org/10.1016/j.jenvman.2018.12.065

Singh R, Bhunia P, Dash RR (2019b) Optimization of organics removal and understanding the impact of HRT on vermifiltration of brewery wastewater. Sci Total Environ 651:1283–1293. https://doi.org/10.1016/j.scitotenv.2018.09.307

Srivastava AKA, Nair A, Ram S, Agarwal S, Ali J, Singh R, Garg MC (2021) Response surface methodology and artificial neural network modelling for the performance evaluation of pilot-scale hybrid nanofiltration (NF) and reverse osmosis (RO) membrane system for the treatment of brackish ground water. J Environ Manag 278:111497

Taha A, Joshi H, Garg M, Manhee H (2021) Case study of evaluation ro desalination systems for potable water in Safwan, Iraq. J Geosci Environ Protect 09:158–181

Tao H-C, Lei T, Shi G, Sun X-N, Wei X-Y, Zhang L-J, Wu W-M (2014) Removal of heavy metals from fly ash leachate using combined bioelectrochemical systems and electrolysis. J Hazard Mater 264:1–7

Thilagavathy P, Santhi T (2013) Sorption of toxic Cr (VI) from aqueous solutions by using treated acacia nilotica leaf as adsorbent: Single and binary system. BioResources 8:1813–1830

Tziritis E, Kelepertzis E, Korres G, Perivolaris D, Repani S (2012) hexavalent chromium contamination in groundwaters of Thiva Basin, Central Greece. Bull Environ Contam Toxicol 89:1073–1077

Wang Z, Feng Y, Hao X, Huang W, Feng X (2014) A novel potential-responsive ion exchange film system for heavy metal removal. J Mater Chem A 2:10263–10272

Wang H, Song X, Zhang H, Tan P, Kong F (2020) Removal of hexavalent chromium in dual-chamber microbial fuel cells separated by different ion exchange membranes. J Hazard Mater 384:121459

Wei X, Kong X, Wang S, Xiang H, Wang J, Chen J (2013) Removal of heavy metals from electroplating wastewater by thin-film composite nanofiltration hollow-fiber membranes. Ind Eng Chem Res 52:17583–17590

Wilbur S, Abadin H, Fay M, Yu D, Tencza B, Ingerman L, Klotzbach J, James S (2012) Agency for toxic substances and disease registry (atsdr) toxicological profiles. Toxicological Profile for Chromium. Atlanta (GA): Agency for Toxic Substances and Disease Registry (US)

Yadav V, Ali J, Garg Manoj C (2021) Biosorption of methylene blue dye from textile-industry wastewater onto sugarcane bagasse: response surface modeling, isotherms, kinetic and thermodynamic modeling. J Hazard Toxic Radioactive Waste 25:04020067

Ying Z, Ren X, Li J, Wu G, Wei Q (2020) Recovery of chromium(VI) in wastewater using solvent extraction with amide. Hydrometallurgy 196:105440

Yunus ZM, Al-Gheethi A, Othman N, Hamdan R, Ruslan NN (2020) Removal of heavy metals from mining effluents in tile and electroplating industries using honeydew peel activated carbon: A microstructure and techno-economic analysis. J Clean Prod 251:119738

Zheng S, Jiang W, Rashid M, Cai Y, Dionysiou DD, O'Shea KE (2015) Selective reduction of Cr (VI) in chromium, copper and arsenic (CCA) mixed waste streams using UV/TiO2 photocatalysis. Molecules 20:2622–2635